Optimization of T-shaped waveguide branches in two-dimensional photonic crystals

Lin Huang (黄 琳), Bing Chen (陈 兵), Yongdong Li (李永东)*, and Chunliang Liu (刘纯亮)

Key Laboratory of Physical Electronics and Devices of the Ministry of Education, Xi'an Jiaotong University, Xi'an 710049, China

**Corresponding author: leyond@mail.xjtu.edu.cn*

Received April 2, 2011; accepted May 28, 2011; posted online August 24, 2011

The interval and the radius of a pair of defect dielectric rods in waveguide channels near the branching region of a T-shaped waveguide branches are simultaneously varied, and their effects on the transmission properties are investigated using the finite-difference time-domain (FDTD) method. Numerical results show that there is an optimized region where the relative bandwidth of high-transmission (total transmittance $\geqslant$0.95) band of the branches is larger than 17%, which is higher than that of the existing same structures (11.60%) with fixed interval. These results provide for engineering application of simple T-shaped waveguide branches with high transmission.

OCIS codes: 130.1750, 230.1360, 230.7370, 250.5300.

doi: 10.3788/COL201210.011301.

Optical waveguide branches play an important role in integrated optical circuits. Such devices are used to divide the input energy equally into two output waveguides without significant reflection and radiation losses. With the development of photonic devices and microminiaturization of integrated optical circuits, wide-angle optical waveguide branches are urgently needed[1−3].

Based on the line-defect waveguides in two-dimensional (2D) photonic crystal composed of a square array of dielectric cylinders, a T-shaped (180°) photonic-crystal waveguide branch can be constructed. However, in general, in order to achieve high-efficiency transmission (high transmission, and low reflection and radiation losses), the branching region of the T-branch must be optimized. Currently, two optimization methods are available: (1) point-defect optimization method based on one-dimensional (1D) scattering theory[3,4]; (2) topology-optimization method[5,6]. The topology optimization method can realize high transmission over wide frequency ranges; however, its optimized structures are irregular and very complex. The optimized structures of the point-defect optimization method are simple; however, the bandwidth of high transmission is usually narrow.

Fan *et al.* adjusted the radius of a pair of defect dielectric rods with a fixed interval introduced into the waveguide channels near the branching region of the T-shaped waveguide branches, thereby achieving lossless transmission in narrow frequency ranges[4]. This simple structure is widely adopted[7−10]. Based on Ref. [4], the radii of N ($16\geqslant N\geqslant 4$) rods in the branching region were adjusted, and the effects of their distribution on the transmission were investigated[11−13]; optimized structures with the wider frequency ranges for high-efficiency transmission were obtained. However, these optimized structures were also irregular and complex.

The transmission characteristics of the T-branch in Ref. [4] indirectly depended on the structure of the branching region (regarded as a resonant cavity). Because the intervals and the radii of the defect rods in the branching region affect the performance of the regarded resonant cavity, they also affect the transmission of the T-branch. Therefore, if the interval and the radius of a pair of defect rods are simultaneously adjusted corresponding to the different resonant cavities, the high-efficiency transmission band could be wider than that in Ref. [4].

In this letter, the relative bandwidth of high-efficiency transmission band of the T-branch in Ref. [4] is set as the optimization objective. Then, by simultaneously adjusting the interval and the radius of a pair of defect rods, their effects on the transmission characteristics are investigated. Finally, the set-optimized parameter for T-branch is obtained, and some important conclusions are drawn.

Figure 1(a) is the schematic view of the photonic-crystal line-defect waveguide in 2D square-lattice made of dielectric cylinders with refractive index n_2 and radius r, which are embedded in the background medium with refractive index n_1. In numerical simulation, let n_1=1 (air), n_2=3.4 (GaAs), and r=0.2a, where a is the lattice constant. The line-defect waveguides are introduced by removing rows of rods in the crystals.

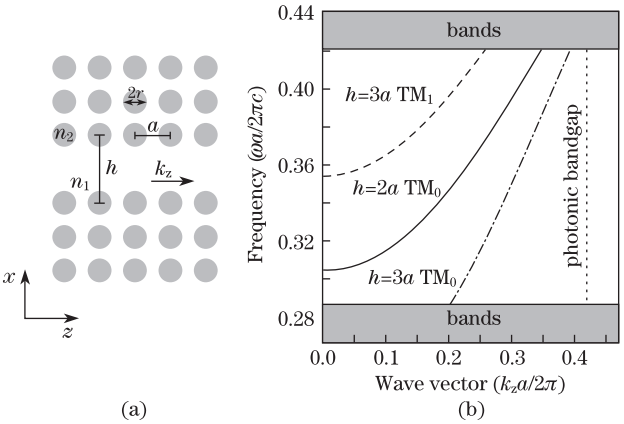

Fig. 1. (a) Schematic view of line-defect waveguide in 2D square-lattice photonic crystals. n_1=1, n_2=3.4, r=0.2a, and k_z is the wave-propagation direction; (b) dispersion curves of guiding modes with different h.

Figure 1(b) is the dispersion curves of different modes under different widths of the waveguide. Plane-wave expansion method[14] based on an $a\times(17a+h)$ supercell is employed to calculate the dispersion properties of such waveguides, where h is the width of the waveguide. Thirty-two grid points are used to represent each lattice constant. The results show that, for transverse magnetic (TM) mode[15], the first photonic band gap of bulk 2D photonic crystals appears between $0.2864(\omega a/2\pi c)$ and $0.4203(\omega a/2\pi c)$. When h=2a (removing a row of dielectric rods), the frequency range of the zero-order TM mode (TM_0) is (0.3043–0.4203)$(\omega a/2\pi c)$, corresponding to relative bandwidth of 32.02%. When h=3a (removing two rows of dielectric rods), the frequency range TM_0 is (0.2864–0.3543)$(\omega a/2\pi c)$, corresponding to relative bandwidth of 21.20%. Obviously, the relative bandwidth for h=2a is higher than that for h=3a; therefore, the width of the line-defect waveguide in T-shaped photonic-crystal waveguide branches is set as h=2a.

Figure 2(a) is the schematic view of the T-shaped waveguide branches based on 2D square-lattice photonic crystals. The computational cell is 121a× 181a. Figure 2(b) is the detailed illustration of 5 × 5 dielectric rods in the waveguide channels near the branching region (as indicated in the dashed box of Fig. 2(a)). A pair of symmetrical defect GaAs rods in waveguide channels is placed in the branching region, and the interval and the radius of the defect dielectric rods are d and r_t, respectively. The interval and the radius of defect dielectric rods are simultaneously varied, and their effects on transmission properties are studied by using the finite-difference time-domain (FDTD) method[16]. The perfect-matched-layer absorbing boundary conditions[16] are adopted on the four boundaries of the calculation region. Firstly, the input and reflection pulses from the branch in time domain are monitored at observation point A, whereas the output signal transmitted through the branch is monitored at observation points B and C. Next, the reflection and transmission spectra are normalized by the input spectrum to achieve normalized reflection and transmission spectra, respectively. Finally, the sum of the normalized transmittance recorded at points B and C is defined as total transmittance (denoted as T), and the frequency band corresponding to $T \geqslant 0.95$ is defined as the high-transmission band, whose relative width is an optimization goal in the following research.

For the T-shaped waveguide branches shown in Fig. 2, the total transmittance T is affected by both d and r_t as a function $T(d, r_t)$. Figure 3 shows the variations of the relative width of high-transmission band along with d and r_t, and there is an optimized region with the relative width of high-transmission band higher than 17% for d and r_t. For practical applications, Fig. 3 can be used to set the optimized parameters for d and r_t. When (d, r_t) is set in such region with relative bandwidth higher than 17%, the T-shaped waveguide branches would achieve a high-relative width of high-transmission band.

Figure 4 shows how the relative width of the high-transmission band varies with d for three different fixed r_t (0.05a, 0.07a, or 0.09a). Figure 4 also shows that there is a maximum value for each fixed r_t, and the maximum value of the relative bandwidth for r_t=0.07a is higher than that for r_t=0.05a or 0.09a. In Fig. 4,

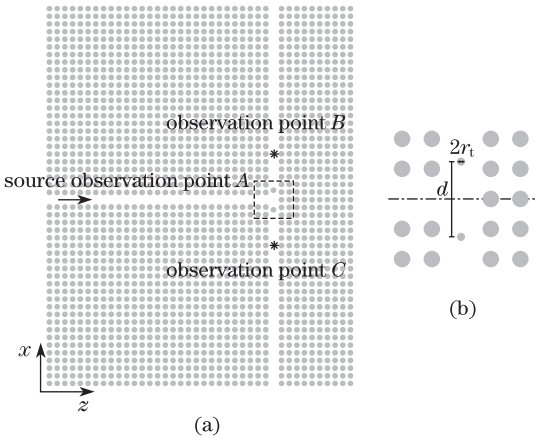

Fig. 2. (a) Schematic view of the T-shaped waveguide branches in 2D square-lattice photonic crystals. The field amplitude is monitored at observation points A, B, and C (asterisks), which are placed in the input and two output ports of the branches, respectively; (b) schematic view of the branching region as indicated in the dashed box of Fig. 2(a); the interval and the radius of defect dielectric rods in the waveguide channels near the branching region are d and r_t, respectively.

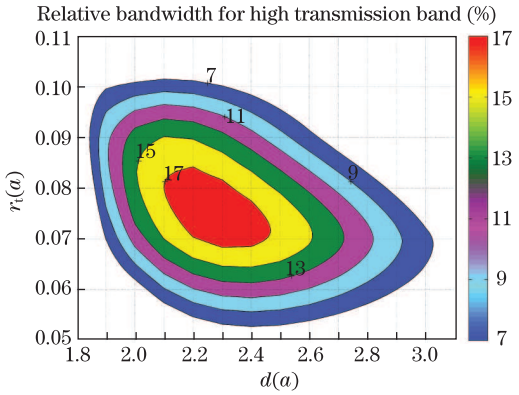

Fig. 3. Relative width of high-transmission band (%) along with d and r_t for T-shaped waveguide branches.

point $A(d, r_t)$=(2a, 0.07a) is the widely adopted parameters[4−7,10,11]. Figure 5(a) is the corresponding transmission, reflection, and losses spectra of the waveguide branches with (d, r_t)=(2a, 0.07a). For the transmission spectrum, the high-transmission band covers a frequency range of (0.3783–0.4249)$(\omega a/2\pi c)$, corresponding to a relative width of 11.60%. For the reflection spectrum, the normalized reflectance is near 0.04. In contrast, point B in Fig. 4 is (d, r_t) = (2.3a, 0.07a). Figure 5(b) is the corresponding transmission, reflection, and losses spectra of the waveguide branches with (d, r_t) =(2.3a, 0.07a). For the transmission spectrum, the high-transmission band covers a frequency range of (0.3490–0.4144)$(\omega a/2\pi c)$, corresponding to a relative width of 17.13%. For the reflection spectrum, the normalized reflectance is near 0.015, which is much less than that in (2a, 0.07a). To sum up, we can realize an obvious increase of the relative width of high transmission when d is varied from 2a to 2.3a; therefore, simultaneously adjusting d and r_t would have better results than only adjusting r_t in the optimization of T-shaped waveguide branches.

In Fig. 6, E_y field distribution in the branching region is plotted at $0.38(\omega a/2\pi c)$ for the structure with (d, r_t)=(2.3a, 0.07a).

In conclusion, the interval d and the radius r_t of defect dielectric rods in the waveguide channels near the branching region of T-shaped waveguide branches are simultaneously optimized to increase the relative bandwidth of high transmission. A large optimized region for d and r_t is demonstrated. Typically, for T-branches with (d, r_t)=(2.3a, 0.07a), the relative width of high transmission is 17.13%, which is a large increase when compared with the existing T-branches with (d, r_t)=(2a, 0.07a), corresponding to a relative width of 11.60%. This means that the relative bandwidth is increased obviously by varying d from 2a to 2.3a. Such results contribute to the design of photonic-crystal waveguide branches with high performance in engineering application.

The work was partially supported by the National Natural Science Foundation of China under Grant No. 61007027.

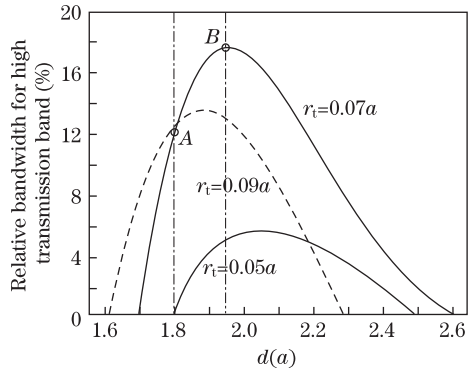

Fig. 4. Curve of the relative width of high-transmission band along with the interval of defect dielectric rods d when r_t is 0.05a, 0.07a, and 0.09a, respectively. Point A: (d, r_t)=(2.0a, 0.07a), point B: (d, r_t)=(2.3a, 0.07a).

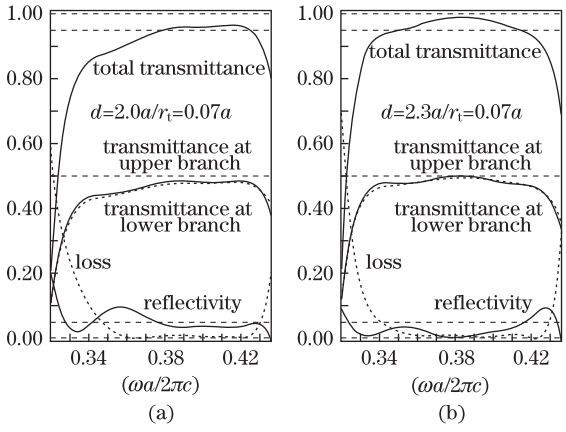

Fig. 5. Transmission spectra (including total transmittance spectrum and transmittance for upper and lower output waveguides), reflection spectra, and losses spectra for T-shaped waveguide branches with different values of d and r_t.

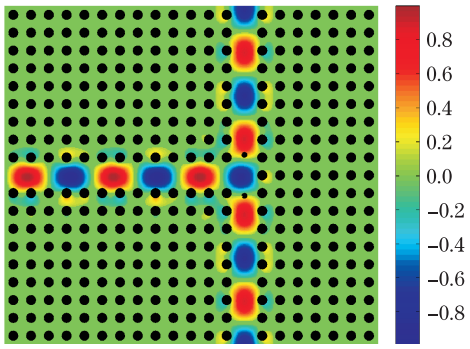

Fig. 6. E_y field distribution in the branching region, at $0.38(\omega a/2\pi c)$, for T-shaped waveguide branches with (d, r_t)=(2.3a, 0.07a).

References

1. J. D. Joannopoulos, P. R. Villeneuve, and S. Fan, Nature **386,** 143 (1997).
2. J. S. Foresi, D. R. Lim, L. Liao, A. M. Agarwal, and L. C. Kimerling, Proc. SPIE **3007,** 112 (1997).
3. J. Yonekura, M. Ikeba, and T. Baba, J. Lightwave Technol. **17,** 1500 (1999).
4. S. Fan, S. G. Johnson, J. D. Joannopoulos, C. Mannolatou, and H. A. Haus, J. Opt. Soc. Am. B **18,** 162 (2001).
5. P. I. Borel, A. Harpoth, L. H. Frandsen, and M. Kristensen, Opt. Express **12,** 1996 (2004).
6. J. S. Jensen and O. Sigmund, J. Opt. Soc. Am. B **22,** 1191 (2005).
7. L. H. Frandsen, P. I. Borel, Y. X. Zhuang, A. Harpøth, M. Thorhauge, M. Kristensen, W. Bogaerts, P. Dumon, R. Baets, V. Wiaux, J. Wouters, and S. Beckx, Opt. Lett. **29,** 1623 (2004).
8. F. Monifi, M. Djavid, A. Ghaffari, and M. S. Abrishamian, J. Opt. Soc. Am. B **25,** 1805 (2008).
9. K. Chung, J. S. Yoon, and G. H. Song, Proc. SPIE **4655,** 349 (2002).
10. J. Zhou, Q. Chang, D. Mu, J. Yang, W. Han, and L. Wang, J. Opt. Soc. Am. B **26,** 2469 (2009).
11. J. Smajic, C. Hafner, and D. Erni, J. Opt. Soc. Am. A **21,** 2223 (2004).
12. W. J. Kim and J. D. O'Brien, J. Opt. Soc. Am. B **21,** 289 (2004).
13. W. Yang, X. Chen, X. Shi, and W. Lu, Phys. B Condens. Matter **405,** 1832 (2010).
14. S. Johnson and J. Joannopoulos, Opt. Express **8,** 173 (2001).
15. J. D. Joannopoulos, S. G. Johnson, J. N. Winn, and R. D. Meade, *Photonic Crystals-Molding the Flow of Light* (2nd ed.) (Princeton University Press, New Jersey, 2008).
16. A. Taflove and S. C. Hagness, *Computational Electrodynamics: the Finite-Difference Time Domain Method* (2nd ed.) (Artech House, Boston, 2000).